ICAST2014 #004

Aerodynamic Performance of a Spanwise Morphing Trailing Edge Concept

Alexander M. Pankonien[1*], Daniel J. Inman[2]

[1] Ph.D. Candidate, Department of Aerospace Engineering, University of Michigan, Ann Arbor, USA
[2] Collegiate Professor and Chair, Department of Aerospace Engineering, University of Michigan, Ann Arbor, USA

Abstract

The Spanwise Morphing Trailing Edge (SMTE) concept seeks to improve aerodynamic performance for small UAVs by creating a smooth control surface that can achieve complex spanwise variation in camber while eliminating gaps and discontinuities. This work represents the first force and deformation analysis of a morphing wing with a smooth surface and independent spanwise-varying actuation for this scale of aircraft. The SMTE concept was realized via a modular design consisting of twelve alternating active and passive spanwise sections. Each active section consisted of a flexure box aileron, actuated by bending Macro-Fiber Composites, with an embedded flex sensor used for closed-loop positional control. Each passive section was composed of an elastomeric honeycomb skin, reducing bubbling and buckling due to aerodynamic loads while still allowing differential actuation between the active sections. The performance of the SMTE concept was measured on a half-span finite wing of 0.3 meter chord, aspect ratio 6 in a wind tunnel. A six axis load balance measured forces about the root quarter-chord and a motion capture system provided tracking of trailing edge deflections. A reference wing consisting of six servo-driven flaps was also tested for a comparison of the SMTE concept against conventional flap technology. Several uniform and differential actuations were investigated for both wings at different angles of attacked, representing attached and separating flow. The SMTE concept achieved tip displacements of approximately 25% of the servo-driven wing, but achieved comparable change in lift for less drag. When normalized by tip deflections measured by the displacements to obtain control derivatives, the SMTE showed actuation effectiveness of three to five times that of the flapped configuration. Additionally, the SMTE eliminated inboard flap vortices maintaining control derivatives improving control derivative performance, and motivating further studies of the concept at other flow speeds and actuation conditions.

1. INTRODUCTION

Morphing aircraft have sought to recreate and exploit the adaptive mechanisms of flying animals in nature ever since the early designs of orthinopters and gliders. The Wright Brother's flyer utilized cables to smoothly warp the wing for flight control, mimicking, in a sense, the fine deformations of a bird's wing in flight [1]. Since these early beginnings, aircraft design rapidly pursued faster, heavier and more

* Corresponding author, alexmp@umich.edu

maneuverable aircraft. Control surfaces changed from biomimetic morphing designs with flexible wings to rigid, hinged flaps that could bear the larger aerodynamic loads. Still, the base size and design of smaller aircraft was limited largely by a single requirement, the necessity of a pilot.

The recent growth in Unmanned Aerial Vehicles (UAVs) has come about as the result of computerization and better communication technology, allowing the pilot to be removed from the aircraft, or from the controls entirely via autonomous aircraft. The result has been a dramatic improvement in duration performance, resulting in many new observation roles, both military and civilian [2]. The number of roles is only expected to increase as the Federal Aviation Administration is expected to issue new rules for the integration of UAVs into commercial airspace in 2015, expecting an annual growth of 12 percent over the next 20 years, demanding further developments in performance [3].

Previously, smooth variation of cambered trailing edges as control surfaces have been investigated for transonic aircraft, seeking to improve aerodynamic performance for long distance flight. This interest was motivated by the promise of small reductions in drag at cruise that could result in large fuel savings, such as a 3.3% improvement in the lift to drag ratio saving 64,000 gallons per aircraft per year for a passenger transport aircraft [4]. The Smart Wing program investigated a smooth morphing trailing edge for a transonic sensorcraft that provided adequate control authority as well as low observability [5]. FlexSys is currently investigating the use of a smooth servo-driven trailing edge for implementation in a business jet [4] . Still, recent studies have shown relatively little impact on performance of conformal morphing of a trailing edge on at the on-design condition, i.e. cruise, compared to conventional actuators, likely as a result of wing design optimization for high efficiency at cruise conditions [6].Accordingly, an ideal mission for the application of a smooth morphing wing would involve sudden requirement changes.

Smaller, subsonic UAVs represent an ideal morphing application as their flight speeds are much closer to ambient wind speed. Thus, small UAVs can experience more extreme control use while attempting to adapt to ambient conditions. Improving the effectiveness of control surfaces for this scale aircraft then has increased relevance as the penalties from adapting to off-design (typically cruise) flight conditions can be more severe.

1.1 Scope of the paper

This paper details the development and initial performance evaluation of a smooth morphing trailing edge (SMTE) control surface for implementation in low speed ($M<0.1$), high performance UAV. The SMTE concept eliminates the gaps and discontinuities in the wing surface associated with conventional control surface design, seen in Figure 1, while still permitting relatively independent spanwise variation in actuation control. It is expected that a morphing concept that eliminates these discontinuities will provide improved control authority at varying flight conditions compared to conventional control surfaces with reduced aerodynamic losses. This work represents the first force and deformation analysis of a morphing wing with a smooth surface allowing independent spanwise actuation for this scale of aircraft.

The relatively soft structures and sensitivity to small changes at this scale require combinations of non-conventional solutions including anisotropic elastomeric honeycombs, as well as smart materials that integrate structure and actuator. The associated methods for control and nonintrusive measurement of these structures are also described. The performance of the morphing concept is compared via experimental testing against discrete flap actuation for a representative half-span, finite wing in a wind tunnel. The results will show that even for smaller trailing edge deflections, the morphing aileron provides comparable control actuation at certain flight conditions, with reduced drag penalties.

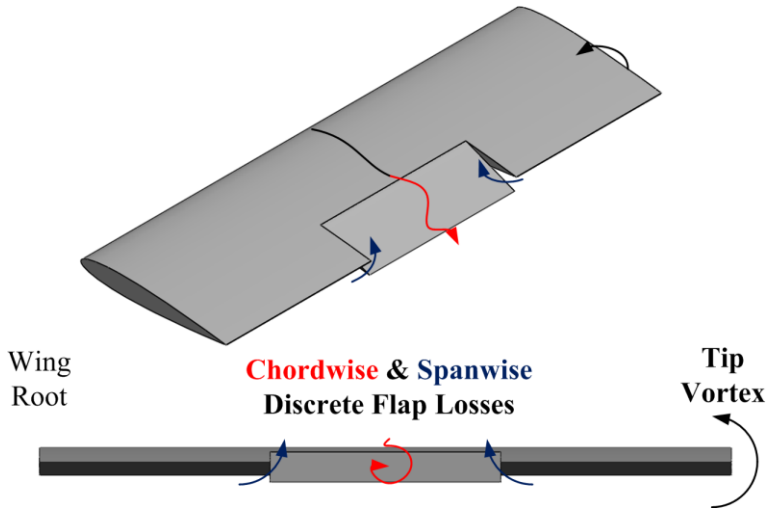

Figure 1. Illustration of chordwise and spanwise losses due to discrete flap actuation

2. MORPHING CONCEPT DESIGN AND CONSTRUCTION

2.1 Description of the Smooth Morphing Trailing Edge concept

The Smooth Morphing Trailing Edge (SMTE) concept was initially developed for fine spanwise control of aerodynamic forces with lessened drag penalty for a UAV wing [7]. The design sought to smooth vary the camber of the trailing edge control surface of a wing or tail, achieving complex spanwise variation while eliminating gaps and discontinuities. The resultant shape would improve aerodynamic force control performance by reducing losses while still permitting spanwise variation in actuation to optimally control aerodynamic forces by arbitrary spanwise variation of camber, shown in Figure 2a.

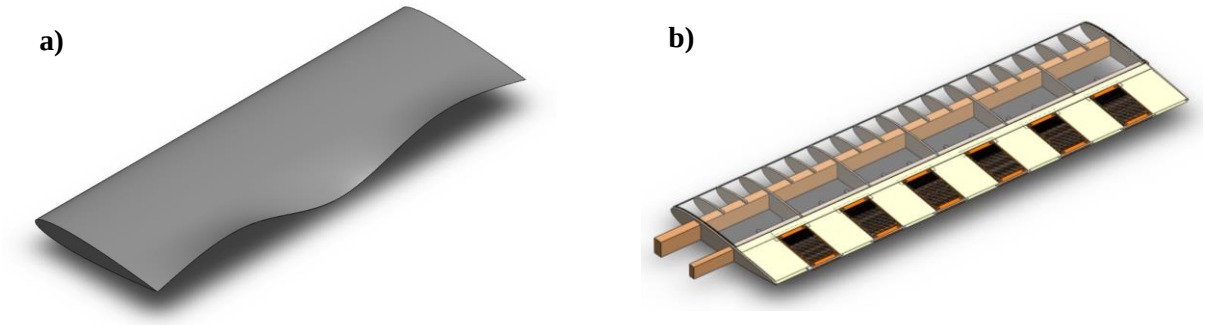

Figure 2. a) Smooth Morphing Trailing Edge concept
b) Modular design of actuators and passive sections

The method chosen for implementation of this concept was a modular section that could be repeated spanwise alternating between active control surfaces and passive sections, shown in Figure 2b. The passive sections consisted of anisotropic patches that stretched between the actuated sections while resisting the deforming effects of aerodynamic loads. This design allowed for repeated integration of a two-dimensional morphing concept and independent design of the skin that would span the gap between the active sections.

The morphing trailing edge actuation concept chosen for implementation in the active sections was the cascading bimorph concept developed by Bilgen *et al.* 2011 [8]. This concept utilizes an internal compliant mechanism actuated by bending smart material actuators, driven by Macro-Fiber-Composites (MFCs) to bend the trailing edge of an airfoil providing smooth chordwise camber variation. These MFCs represent an ideal morphing actuator for this scale due to the integration of structure and actuator into a single structure representing minimal addition in complexity or mass. This concept was adapted into a repeatable modular section produced by multi-material additive manufacturing for precise and repeatable control over the compliant structure features and stiffness properties creating the Flexure Box morphing aileron [7]. This design also permitted inclusion of embedded sensors for positional measurement and closed-loop control.

The anisotropic passive section for use between the morphing actuators was also developed by Pankonien *et al.* 2013 as a stretchable skin with embedded elastomeric honeycomb [7]. A representative SMTE test article composed of two active sections and one passive section was tested for the impact of different skins on actuation range and deformation due to aerodynamic loads. The honeycomb increased out-of-plane stiffness to aerodynamic loads as compared to a simple elastomeric skin and it also permitted tailorable in-plane compliance for differential control surface actuation. The honeycombs were constructed via elastomeric additive manufacturing to improve control over the geometry, material properties while improving repeatability and speed of prototyping design changes.

2.2 Construction of morphing and discrete flap wings

Although the previous test of the representative section allowed for a preliminary assessment of the authority of the actuators under aerodynamic loads, the resultant control configurations were limited by the number of actuators used, namely 2. Modelling the three-dimensional flow about the compliant section was deemed to be prohibitive in complexity due to the number of disciplines involved including smart materials, soft materials, and viscous flow. Accordingly, an experimental test for differential spanwise actuation was determined to allow for an initial assessment of performance capabilities. A finite wing was chosen to investigate the ability of the SMTE concept to adapt to spanwise changes in flow and separation at different flight conditions. Differing spanwise flow scenarios corresponding to different flight conditions could then be created by varying the angle of attack of the wing.

The modular wing morphing wing shown in previously in Figure 2b, was constructed for a half-span finite wing with NACA 0012 airfoil and a chord of 0.305 meters with 6 active sections. Including a 0.14 meter cowling at the root for mounting, the wing had semi-span of 0.91 meters resulting in an aspect ratio of 6. Prior investigation of the Flexure box morphing aileron showed that the lighter “unimorph” version utilizing only two MFCs was suitable for characterization of the concept up to approximately 15 m/s [9]. Accordingly, for simplicity of implementation, only two MFCs were utilized in each active section, consistent with previous work. Each active section consisted of an M-8557-P1 MFC from Smart Material Corporation, which is approximately 6.4 cm in active width. Each active section was spaced approximately 12.8 cm apart spanwise, creating an effective 50% distribution of active and passive material over the span of the airfoil.

The skin was constructed with an elastomeric honeycomb, which was adhered to a 0.25 mm thick silicone sheet with a two-part silicone mixture via a micrometer film applicator. The stretchable trailing edge of the morphing skin was created by bonding two sides together for the last 0.6 cm of the chord using the same two-part silicone mixture. The skin was then adhered to the actuators via thin two-sided silicone to cyanoacrylate adhesive tape and was then pre-strained by approximately 10% to the leading edge where it was secured by high-strength adhesive. The construction of the morphing wing is shown in Figure 3a with inner honeycombs exposed for comparison with Figure 2b.

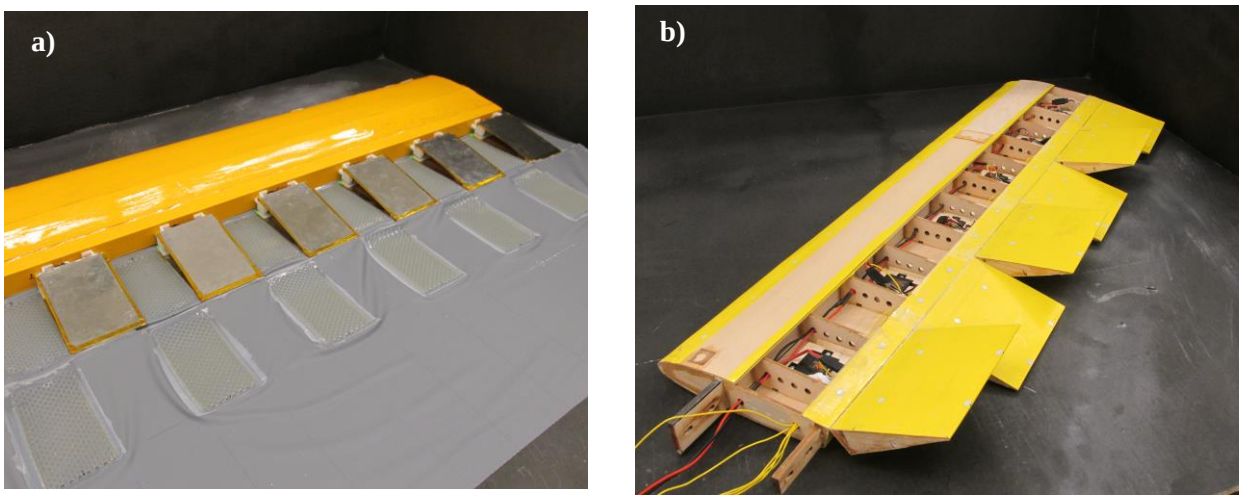

Figure 3. a) Construction of SMTE Wing with inactive honeycombs and active MFC sections
b) Servo distribution and hingeline in comparative discrete flap wing

Due to the relatively complexity of the test article, a conventional wing composed of discrete flaps was also constructed to provide a comparative baseline against which improvements of the morphing wing could be identified. The flaps were sized to have a chordwise hingeline equivalent to the beginning of the morphing sections. For consistency of comparison, both wings utilized mostly identical construction methodology forward of the rear spar, creating a stiff wing box via carbon-fiber capped spars with integrated ribs and balsa wood sheeting for a pressure surface and, shown in Figure 3b.

Many efforts were made to minimize the impact of the hinge and servo-arm linkage on the flow and thus provide a fair assessment of the morphing wing with best practices in drag reduction for discrete control surfaces. The flap was hinged along the top surface with no gap consistent with methodology used to minimize gap losses in conventional wings. The control arm was embedded within the airfoil profile surface so as not to cause additional drag. The maximum flap deflection angles of the servos were sized at approximately +/- 25^{o}, consistent with a typical application for UAVs. Although this tip displacement range exceeds that of the capabilities of the morphing wing, for initial assessment and practical comparison the range was not limited. The span of the wing not occupied by the fixed cowling at the root was equally divided into 6 flaps of approximately 14 cm in span with no passive spanning sections. This allowed for a comparison of the morphing concept with a differential discrete flap concept.

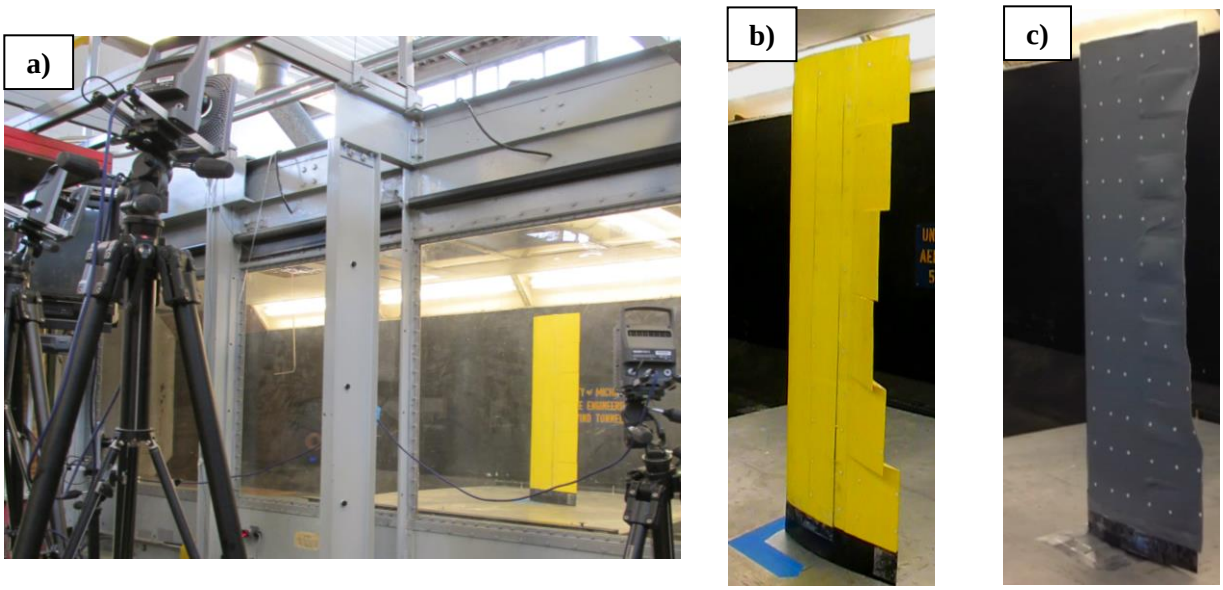

Figure 4. a) Vertically mounted finite wing in wind tunnel with tracking cameras
b) Flap and **c)** SMTE wings with quadratic flap variation (S2)

3. COMPARATIVE WIND TUNNEL TEST

3.1 Setup description

Both finite morphing and discrete flap wings described in section 2 were tested for authority over aerodynamic control forces at varying flight conditions in the 1.5 m x 2.1m wind tunnel at the University of Michigan, seen in Figure 4a. The goal was to measure the improvement in control performance of the SMTE morphing concept over discrete flaps for differing spanwise flow conditions. A single flow speed of 10 m/s, monitored by a hot-wire anemometer in the test section, was chosen to limit the aeroelastic effects on wings.

The aerodynamic forces on the wings were measured about quarter-chord at the root of the wing utilizing a calibrated 6-axis force balance, mounted below the wind tunnel. The wings were mounted vertically in the wind tunnel, directly to the force balance, eliminating the need for a yoke or other mounting device that could interfere with the aerodynamic forces or restrict the actuation of the compliant wing.

3.2 Setup characterization

A ground plate approximately 30 cm from the floor of the wind tunnel was used to remove the wing from the boundary layer of the wind tunnel. The gap between the finite wing and the splitter plate was necessary to ensure the accuracy of the force balance, but was minimized to ensure that it minimally impacted force results by allowing air to flow from the high pressure surface below the wind tunnel to the upper surface. To estimate the quality of the experimental setup, the lift curve slope of both wings was

compared to finite wing theory. The relationship between the lift curve of an infinite-span wing can be related to that of a finite wing by Equation 1, providing an estimate of the accuracy of the results [10]. Here "a_0" represents the two-dimensional lift-curve slope, "AR" the aspect ratio of the wing, and "a" represents the lift-curve slope of the finite wing aspect ratio, and "e" is the Oswald efficiency factor. For an initial estimate, assuming e=1, employing this equation for the provided aspect ratio, and given the lift curve slope of the NACA 0012 airfoil to be approximately 2π, the variation in lift due to angle of attack is expected to be bounded by 75% of the infinite wing value, due to downwash caused by the tip vortex.

$$\frac{a}{a_0} = \frac{1}{1+\frac{a_0}{\pi e AR}} \approx 0.75 \tag{1}$$

Examining the unactuated wing, a several angles of attack ranging from -5° to +5° and applying a linear fit, the slope of the lift curve was found to be 68.3% of the infinite span value, representing less than 10% relative error as expected by finite wing theory, regardless of the spanwise efficiency of actuation. Thus the test setup was determined to provide sufficient accuracy for initial assessment of aerodynamic forces on a finite wing.

3.3 Actuator position control and verification

The discrete flaps were controlled internally by the digital servos to achieve the desired configurations. An Arduino program prescribed the necessary inputs to the servos according to configurations commanded by a National Instruments Data Acquisition device which also recorded time-averaged force balance results. For the morphing wing, the Arduino control program was altered to utilize a time-averaged version of the PID positional control program implemented previously by Pankonien *et al. 2014* to control the trailing edge position via calibrated embedded sensors [9]. Thus, similar to the control program within the servo, each morphing actuator within the SMTE concept continuously sought to reach each commanded position regardless of aerodynamic forces or the effects of the other actuators as conveyed by forces through the skin.

Positional data for the wings was measured non-intrusively via circular reflective markers, seen in both Figure 4b and 4c, which were tracked by a VICON motion-capture system. The system consisted of four cameras positioned outside the wind tunnel, three of which are seen in Figure 4a, to independently track the positions of the reflective markers in real-time. This allowed for confirmation during prescribed actuation that the control system had settled actuating to a prescribed configuration. Once a configuration was achieved the time-average positional data of the wing and resultant aerodynamic forces.

3.4 Test description

Two angles of attack, 5° and 10°, were chosen to represent an attached and near-stall flight condition, respectively, with significant spanwise flow from the tip vortex. To identify the capabilities of the two concepts to affect aerodynamic loads, several different spanwise variations in actuation were tested at each flight condition. Eight uniform and three spanwise-varying actuation configurations, shown in Figures 5 and 6 respectively, were chosen to study the ability of the two wings to control aerodynamic forces at the different flight conditions. These figures show the equivalent angle and tip displacement of the configurations.

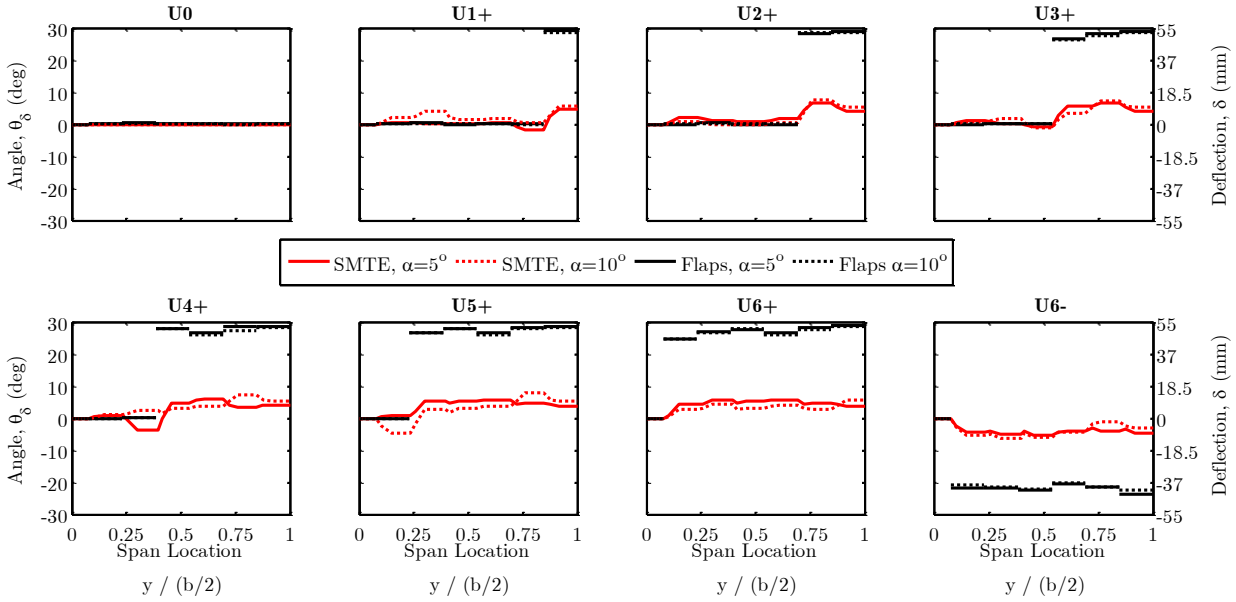

Figure 5. Uniform actuation configurations for SMTE and discrete flaps wings

The eight uniform actuation configurations were chosen to study the effect of increasing the relative span of the control surface on actuator effectiveness. Thus, the actuations studied used an increasing number of actuators at their maximum possible actuation. The unactuated configuration, U0, served as a baseline for comparison of aerodynamic forces between the two concepts. For simplicity of reduction in test parameters, only the maximum allowable actuations were tested for each wing. Positive actuation was the focus of investigation, representing an increase in lift beyond the baseline caused by the positive angle-of-attack of the testing conditions. Thus configurations U1+ through U6+ were tested to symbolize an increasing-span flap or morphing surface. Configuration U6- was chosen as a mirror-case for U6+ to investigate alleviation of aerodynamic loads.

Clearly, the conventional servo-driven flaps command significantly larger tip-deflections, however, the relatively smooth variation of camber and spanwise actuation are expected to provide improved relative actuation over the discrete flaps. The variations in position between the configurations at the different angles of attack are a result of positioning errors in the control system as the actuators attempt to compensate for aerodynamic loading.

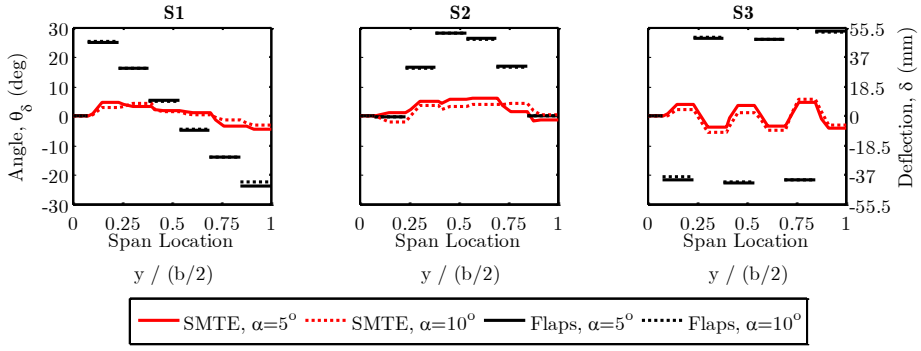

Figure 6. Spanwise-varying actuation configurations for SMTE and discrete flaps wings

The three spanwise actuation configurations chosen were a linear, quadratic, and sinusoidal spanwise variation, shown in Figure 6. These configurations were symmetric about the spanwise-distribution of actuators and did not "adapt" to the downwash caused by the tip vortex, but rather were prescribed actuations. Configurations S1 and S3 were expected to generate no net change in lift or roll moment but large changes in drag due to their symmetry about U0. Configuration S2 was expected to generate lift, but with reduced losses in the flapped wing due to the gradual spanwise actuation.

3.5 Force results

The variation of forces created by the flaps at the tested flight conditions are summarized in Figure 7. Beginning with the flapped wing, it can be seen that increasing spanwise flaps (U0 → U6+) result in a positive change in lift. Configurations U4+ to U5+ show no increase in lift or pitching moment even as more flaps are actuated. Finally, configuration U6 + represents a slight decrease in roll moment, even as lift increases, showing the effects of tip stall. Additionally, the drag rise associated with actuating all flaps at this condition is significantly higher.

Comparatively, the morphing wing is just as effective at increasing lift for attached flow at 5^{o} with decreased drag, although the effect on rolling moment is not as large, probably because the lift for the flapped wing has been shifted comparatively outboard due to inboard vortices associated with actuation. The relatively lower pitching moment associated with the morphing actuation can also be explained due to decreased drag associated with the morphing actuation.

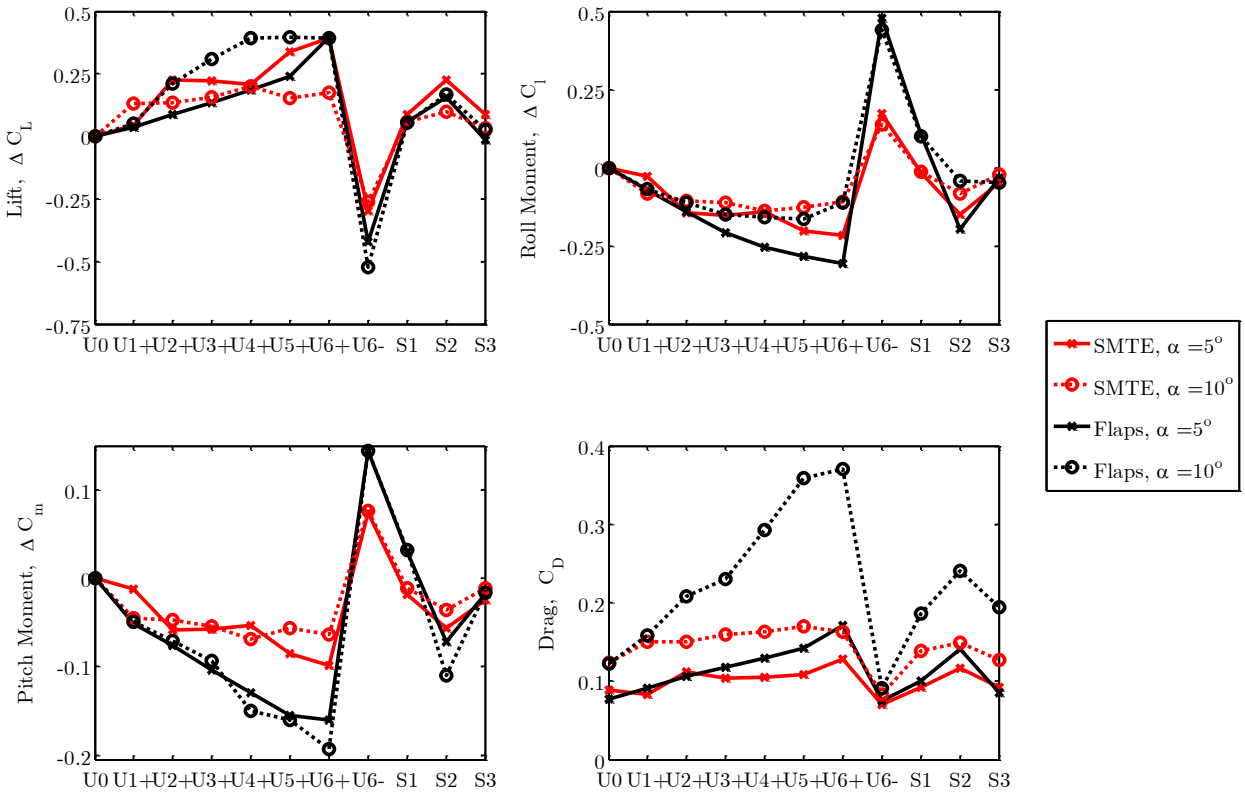

Figure 7. Spanwise-varying configurations for SMTE and discrete flaps wings

Examining the spanwise-varying configurations, S1 and S3 are seen to effectively produce drag with very low lift, pitching or rolling moment, corresponding to a "braking mode". These braking configurations are more effective at 10° at producing drag, especially for the flapped case. For a closer examination of the effectiveness of these configurations, a relative metric must be established.

3.6 Control derivatives

A metric was devised to compare the effectiveness of the two wings over the different actuation configurations. As a common feature of both wing designs, the average of the magnitude of the tip displacement for each configuration was used to summarize control authority. The nondimensional forces could then be normalized by the tip displacements to create an effective partial derivative of control forces, a relevant metric in aircraft control design. The control derivatives were established by dividing the change in nondimensional force by the integral of the absolute value of the tip displacements. An example calculation method for lift is shown in Equation 2 and the results are summarized in Figure 8.

$$\left|C_{L_\delta}\right| = \left|\frac{\partial C_L}{\partial \delta_{tip}}\right| \quad \approx \quad \frac{\left|\Delta C_L\right|}{mean\left|\delta_{tip}\right|} = \frac{\left|\Delta C_L\right|}{\int_{\bar{y}=0}^{\bar{y}=1}\left|\delta_{tip}\right| d\bar{y}} \tag{2}$$

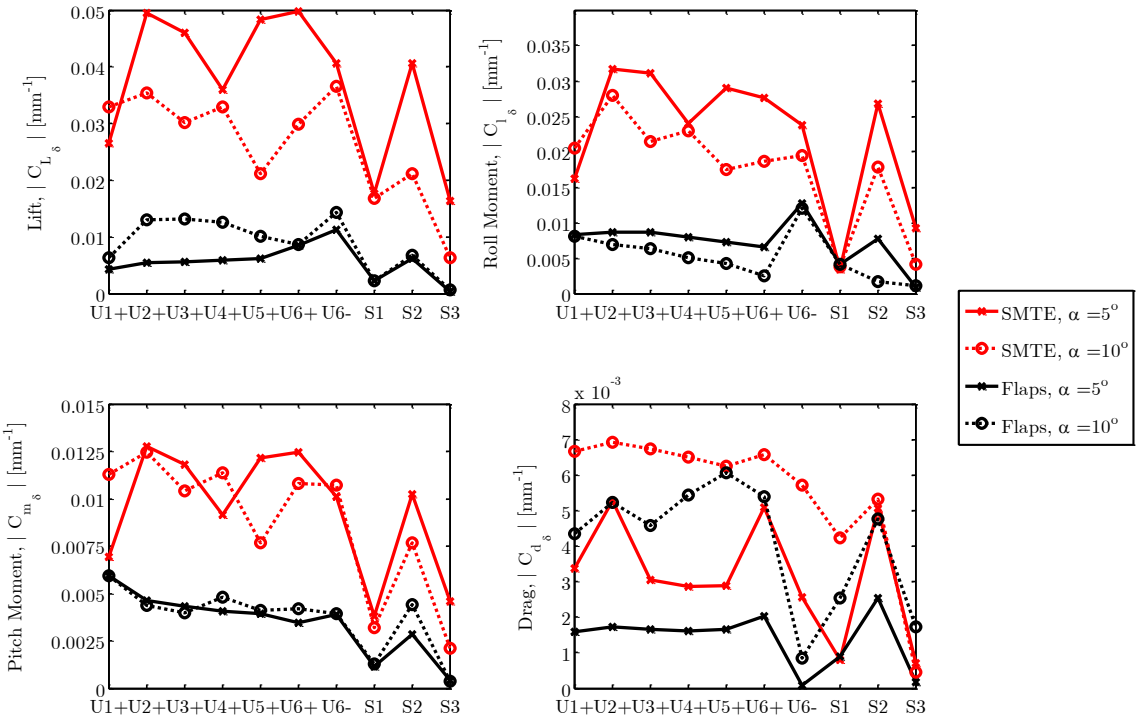

Figure 8. Effectiveness of control surfaces for various aerodynamic forces

By examining the control derivataives, the previous result becomes more apparent as the size of the flap increases in span its effectiveness increases for 5^o. It is expected that this effect is caused by the inboard vortex caused by flap actuation which decreases in relative effect as the span of the flap is increased. However, at 10^o angle of attack, the marginal gain in lift decreases as flap size increases as stall limits the maximum lift generated. For the morphing wing, no such trend is seen in lift, due to the lack of inboard vortex and the suppression of separation by the smooth shape change. Another interesting conclusion shown is that none of the spanwise-varying configurations show an improvement in control authority beyond that of uniform actuation. Although, the S2 configuration is comparable with uniform actuation and could be useful for integration into a wing where both spanwise boundaries of the flap are required to be fixed. This result is expected as the tested configurations were not informed by a model.

Comparing the magnitude of the control derivatives between the two wings, it can be seen that the SMTE exhibits much greater control over forces for lift and rolling moment (approximately 3 to 4 times) when normalized by tip displacement, but only one to two times as much in drag and pitching moment. Clearly, closer analysis between the wings would be assisted by matching the tip displacements of the two concepts, but this result also motivates morphing designs with larger deflection ranges to further capitalize on this expected improvement due to a smooth surface.

5. SUMMARY AND CONCLUSIONS

This paper detail the development and initial performance evaluation of a smooth morphing trailing edge (SMTE) control surface for performance improvement of a low speed (M<0.1) UAV. This design sought to reduce the aerodynamic losses associated with adapting to varying flight conditions by creating arbitrary spanwise-varying camber along the trailing edge of the aircraft, free of discontinuities. The morphing concept was realized via a modular concept for a 0.9 m chord finite wing consisting of twelve alternating active and passive sections. The active sections were driven by conformally bending MFCs and the passive sections were made with anisotropic honeycombs bonded to a prestrained skin. A comparative wing composed of servos and six differentially-actuating flaps was constructed for comparison with the morphing design. Both wings were tested in a wind tunnel at two different angles of attack, 5^o and 10^o for a flow speed of 10 m/s, representing attached and separating flow flight conditions. At these two conditions, the aerodynamic control forces and tip displacements of both wings were measured and compared for eleven different actuation configurations.

The results showed that for attached flow, increasing the span of a flapped wing improved the relative performance by decreasing the relative effect of the inboard flap vortex. However, for separating flow, increasing the flap span did not strictly increase lift control, but simply resulted in increased drag. The morphing wing did not show either of these effects, exhibiting the benefit of a smooth morphing surface to eliminate spanwise losses due to actuation while better controlling separation. Additionally, for attached flow, the morphing wing achieved comparable change in lift for less drag. Although the flap actuations were much larger, resulting in a larger range of control forces, the morphing wing was calculated to exhibit greater control authority when normalized by tip displacement. This test warrants further investigations for matched tip displacements of the morphing and discrete flapped wing.

ACKNOWLEDGEMENTS

The authors are grateful to the University of Michigan and the Clarence L. “Kelly” Johnson collegiate professorship for the fellowship funding that made this research possible. The authors would also like to thank Associate Professor Anouck Girard for the collaborative use of the positional tracking system.

REFERENCES

1. Valasek, J., *Morphing Aerospace Vehicles and Structures*, Wiley, 2012, doi:10.1002/9781119964032.ch1 .

2. Bekmezci, I., Sahingoz, O.K., and Temel, A., "Flying Ad-Hoc Networks (FANETs): A survey," *Ad Hoc Networks*, Vol. 11., No. 3, 2013, pp. 1254–1270, doi: 10.1016/j.adhoc.2012.12.004 .

3. "FAA Aerospace Forecast Fiscal Years 2012-2032 ," <https://www.faa.gov/about/office_org/headquarters_offices/apl/aviation_forecasts/aerospace_forecasts/2012-2032/> , accessed 8 July 2014.

4. Kota, S., Osborn, R., Ervin, G., Maric, D., Flick, P., and Paul, D., "Mission adaptive compliant wing-design, fabrication and flight test," *Morphing Vehicles, number RTO-MP-AVT-168-18 in. NATO Research and Technology Organization*, 2009.

5 . Kudva, J., "Overview of the DARPA smart wing project," *Journal of Intelligent Material Systems and Structures*, Vol. 15, No. 4, pp. 261-267, 2004, doi:10.1177/1045389X04042796 .

6. Lyu, Z., and Martins, J.R.R.A., "Aerodynamic Shape Optimization of an Adaptive Morphing Trailing Edge Wing," *Proceedings of the 15th AIAA/ISSMO Multidisciplinary Analysis and Optimization Conference*, Atlanta, GA, 2014, doi:10.2514/6.2014-3275 .

7. Pankonien, A., and Inman, D.J., "Experimental testing of spanwise morphing trailing edge concept," *Proceedings of SPIE - The International Society for Optical Engineering*, Vol. 8688, pp. 1-15, 2013, doi :10.1117/12.2009400 .

8. Bilgen, O., Kochersberger, K.B., Inman, D.J., and Ohanian III, O.J., "Novel, bidirectional, variable-camber airfoil via macro-fiber composite actuators," *Journal of Aircraft*, Volume 47, No. 3, pp. 303–314, 2010, doi:10.2514/1.45452 .

9. Pankonien, A.M., and Inman, D.J., "Aeroelastic performance evaluation of a flexure box morphing airfoil concept," *Proceedings of SPIE - The International Society for Optical Engineering*, Vol. 9057, pp. 1-14, 2014, doi:10.1117/12.2046406.

10. Anderson, J.D., *Fundamentals of Aerodynamics*, McGraw-Hill, pp. 312-323, 2010 .